Published in final edited form as:
J Mater Chem. 2012 January 1; 22(43): 22888–22898. doi:10.1039/C2JM32466K.

An Investigation of Siloxane Cross-linked Hydroxyapatite-Gelatin/Copolymer Composites for Potential Orthopedic Applications†

Jason Christopher Dyke[1], **Kelly Jane Knight**[1], **Huaxing Zhou**[1], **Chi-Kai Chiu**[2], **Ching-Chang Ko**[2,*], and **Wei You**[1,*]

[1]Department of Chemistry, University of North Carolina at Chapel Hill, Chapel Hill, NC 27599-3290

[2]Department of Orthodontics and Applied Materials Sciences Program, University of North Carolina at Chapel Hill, Chapel Hill, NC 27599-7450

Abstract

Causes of bone deficiency are numerous, but biomimetic alloplastic grafts provide an alternative to repair tissue naturally. Previously, a hydroxyapatite-gelatin modified siloxane (HAp-Gemosil) composite was prepared by cross-linking (*N*, *N*′-bis[(3-trimethoxysilyl)propyl]ethylene diamine (enTMOS) around the HAp-Gel nanocomposite particles, to mimic the natural composition and properties of bone. However, the tensile strength remained too low for many orthopedic applications. It was hypothesized that incorporating a polymer chain into the composite could help improve long range interaction. Furthermore, designing this polymer to interact with the enTMOS siloxane cross-linked matrix would provide improved adhesion between the polymer and the ceramic composite, and improve mechanical properties. To this end, copolymers of L-Lactide (LLA), and a novel alkyne derivatized trimethylene carbonate, propargyl carbonate (PC), were synthesized. Incorporation of PC during copolymerization affects properties of copolymers such as molecular weight, T_g, and % PC incorporation. More importantly, PC monomers bear a synthetic handle, allowing copolymers to undergo post-polymerization functionalization with graft monomers to specifically tailor the properties of the final composite. For our investigation, P(LLA-*co*-PC) copolymers were functionalized by an azido-silane (AS) via copper catalyzed azide-alkyne cycloaddition (CuAAC) through terminal alkyne on PC monomers. The new functionalized polymer, P(LLA-*co*-PC)(AS) was blended with HAp-Gemosil, with the azido-silane linking the copolymer to the silsesquioxane matrix within the final composite.

These HAp-Gemosil/P(LLA-*co*-PC)(AS) composites were subjected to mechanical and biological testing, and the results were compared with those from the HAp-Gemosil composites. This study revealed that incorporating a cross-linkable polymer served to increase the flexural strength of the composite by 50%, while maintaining the biocompatibility of HAp-Gemosil ceramics.

1. Introduction

Natural bone is a lightweight mineral composite consisting of inorganic apatite, mainly hydroxyapatite (HAp), within a dense matrix of organic collagens. The long fibrous collagen

†Electronic Supplementary Information (ESI) available. See DOI:10.1039/b000000x/

*Correspondence should be directed to wyou@unc.edu and koc@dentistry.unc.edu.

Supporting Information Available

^{1}H NMR is available for all previously unpublished monomers and polymers. ^{13}C NMR is provided for PC and AS. GPC traces are provided for all polymers. DSC analysis is given for PLLA, P(LLA-*co*-PC)6.4% and P(LLA-co-PC)21.05%.

makes the normally brittle HAp more resilient, helping to improve flexural strength in natural bone.[1] The hierarchy HAp-collagen structure, however, cannot be reproduced easily using engineering principles. Sequentially, autografts (tissues from the host) have become the gold standard for replacement of damaged tissues.

Due to the drawbacks (e.g., donor site morbidity, shortage of resources) of autografts, the need for alternate alloplastic materials is clear. Orthopedic biomaterials, in particular, have been heavily studied, and comprehensively reviewed by Puppi[2] and Shoichet[3] in greater detail. In particular, significant progress has been achieved in engineering materials capable of degrading *in vivo*, either by hydrolytic or enzymatic activity to promote formation of natural osseous tissue, through growth of tissue into the composite material.[4] This *biodegradable* approach allows for the body to heal itself more gradually, with the scaffold serving as a *temporary* matrix until sufficiently strong osseous tissue can assume a physiological load.[5–6]

In response to the needs, several classes of biocompatible and biodegradable polymers have been established for numerous medical applications. Polyesters such as poly(lactic acid) (PLLA)[7–9], poly(glycolic acid) (PLGA)[10], poly(*ε*-caprolactone) (PCL)[11–12] and poly(trimethylene carbonate) (PTMC)[13–15] have been investigated as native or as in blends[16–17] for a variety of medical applications. Each of these polymers has unique mechanical and degradative properties allowing them to be utilized in a wide range of biomaterials.[2–3,18–21] Though homopolymers have good properties for *in vivo* applications, they are often limited by their diversity in function. Therefore, copolymers present a useful way to obtain tunable properties such as molecular weight, crystallinity, glass transition temperature (T_g), modulus, degradation behavior and tensile strength, all of which can be specifically optimized for use in preparing scaffolds.[10,13] Furthermore, the structure of many of these monomers can be synthetically altered to tailor their properties. These monomers can be combined in nearly endless ways to form functional materials with application specific properties. Because of this, it is important for synthetic chemists to formulate new monomers and design new monomers and polymers in an attempt to improve the utility of materials engineered for specific applications.

Recently, Ko and co-workers created a composite of Hydroxyapatite-Gelatin (HAp-Gel)[22] that mimicked the natural composition and properties of bone[23] and was able to demonstrate promise for *in vivo* and *in vitro* biocompatibility.[24] However, challenges remained in developing useful grafts from these composites because they demonstrated poor processibility and insufficient strength when porous. These problems were ultimately improved by incorporation of an additional cross-linking agent, (*N*, *N*′-bis [(3-trimethoxysilyl)propyl]ethylene diamine (enTMOS).[25] This small molecule is capable of undergoing hydrolysis-condensation of alkoxy-silanes to produce a silsesquioxane matrix within the hydroxyapatite-gelatin modified siloxane (HAp-Gemosil) composite. This helps give additional structural support to the composite and can help impart the network strength of the silane matrix into the composite, leading to enhanced mechanical properties and molding ability. While this matrix did improve the compressive strength and processibility of the composite, the short chain siloxane based matrix was brittle and still susceptible to tensile failure. It was clear that a more robust composite was needed in order to further advance this system for potential scaffolding applications. One possible solution is to design and incorporate a biocompatible and cross-linkable polymer of sufficient chain length into the composite.

First, we chose a copolymer of PLLA and PTMC to blend into Hap-Gemosil composites. PLLA has demonstrated previous success in use with hydroxyapatite ceramic composites,[16,26–27] and PLLA's biocompatibility has long been established. However, at

physiologic temperature, PLLA is brittle and can contribute to low composite strength.[28] Therefore, an amorphous TMC derivative, Propargyl Carbonate (PC), was synthesized and utilized as the co-monomer. This monomer can act to soften PLLA and toughen brittle composites[29], as demonstrated in previous studies where P(LLA-*co*-TMC) copolymers showed a decrease in T_g with increasing TMC incorporation.[30–32] The combination of both properties from PLLA and PPC (a derivatized PTMC) polymer could help P(LLA-*co*-PC) copolymers to exhibit good flexural strength and elongation, ideal for creating a more robust ceramic composite. In addition, both PLLA and PTMC polymers have unique degradative properties, allowing the degradation behavior of future composites of this formulation to be controlled. Finally, from the synthetic perspective, both of these monomers are ideal candidates for ring-opening polymerizations (ROP), whereby byproducts are avoided and polymers of high MW can be readily obtained.[31–33] Since both monomers share a common method of polymerization, copolymer composition is more easily controlled. More importantly, cyclic carbonates can be easily derived[34] and the modifications present on PC would allow the incorporation of a pendant silane graft monomers onto the polymer backbone (*vide infra*), while also imparting similar properties to PTMC.

Second, we designed the chosen copolymer to cross-link within the HAp-Gemosil composite because this would lead to improved tensile strength via better long range interaction when compared with physically blending polymer into the composites. Specifically, this approach – designing polymers with cross-linkable grafts – would provide two advantages: (a) increase interfacial adhesion over polymer blends, and (b) enhance long range interactions when compared with composites that are only cross-linked by small molecules (e.g., enTMOS). Consequently, the composite would more effectively mimic the short and long range chemical interactions seen within bone, thereby improving tensile strength of the composite.[35] This should in turn help to resist tensile loading by distributing forces more evenly through the composite, rather than at the point of application.[36] Since HAp-Gemosil composites were originally cross-linked using an amino-silane (enTMOS), it would be ideal to design the copolymer to bear a similar cross-linkable silane group.

However, the sensitivity of the graft monomer's silane groups precluded their direct incorporation prior to polymerization. Therefore, we employed the CuAAC Chemistry ('Click" reactions) to impart the silane functionality to the polymer via post-polymerization functionalization by quantitatively coupling the graft monomer azide to the main chain alkyne of the polymer backbone.[37–38] Thus the PC monomer was synthesized to bear a pendant acetylene group, while the azide functionality was linked with the silane (e.g., 5-azido-*N*-(3-(trimethoxysilyl) propyl) pentanamide). After the copolymerization of LLA and PC, the terminal alkyne group of the copolymer would easily react with the azido-silane (AS) graft monomer via CuAAC chemistry. This post-polymerization functionalization approach allows the grafting of the silane functionality to occur *after* polymerization, ensuring the fidelity of the silane groups is maintained. P(LLA-*co*-PC)(AS) can then be blended with HAp-Gel and cross-linked in the presence of enTMOS to produce a fully cross-linked composite through hydrolysis – condensation of trialkoxysilyl groups present on both the copolymer and enTMOS. Such programmed composite would improve adhesion through coordination of grafted amide and triazole groups to free carboxylate groups on gelatin and also through silane cross-linking to HAp.

Based on this rationale, we have synthesized and characterized a series of P(LLA-*co*-PC) polymers via Ring-Opening Polymerization (ROP) and functionalized the polymers with pendant silanes. Composites formed by incorporating these polymers with HAp-Gemosil were easily molded and set quickly. To determine the impact of blending P(LLA-*co*-PC)(AS) with HAp-Gemosil, transwell plates were filled with this new composite material and preosteoblasts MC3T3-E1 were cultured in the bottom of these plates for 21 days. It was

observed that throughout this period, the growth curves of cells in the presence of either HAp-Gemosil or HAp-Gemosil/P(LLA-*co*-PC)(AS) composites were very similar, suggesting that the synthesized polymer can help improve mechanical properties without negatively impacting the biocompatibility. In addition, both materials showed similar cellular growth curves to those of the control samples, suggesting these materials provide a suitable substrate for cellular attachment and proliferation. Furthermore, biaxial bending tests were undertaken to determine the impact that incorporating P(LLA-*co*-PC)(AS) into a ceramic composite has on flexural strength. It was also observed that this polymer helped increase fiber bridging within the composite, leading to higher flexural strength than that of non-polymeric HAp-Gel composites. These results suggest that the design of this copolymer, and the use of graft monomers as cross-linking agents possess merit for future study in expanding their applications for bioceramic composites.

2. Experimental Details

General Methods—All moisture sensitive reactions were performed in flame-dried glassware under an atmosphere of Ar. Reaction temperatures were recorded as external bath temperatures. The phrase “concentrated under reduced pressure” refers to the removal of volatile materials by distillation using a Büchi rotary evaporator at water aspirator pressure (< 20 torr) followed by removal of residual volatile materials under high vacuum (< 1 torr). The term “high vacuum” refers to vacuum achieved by a standard belt-drive oil pump (< 1 torr).

^{1}H and ^{13}C NMR spectra were recorded on Bruker AC-400 (400 MHz) spectrometers. Chemical shifts are reported in parts per million (ppm) relative to residual solvent peaks (CHCl3: 1H: d 7.26). Peak multiplicity is reported as: singlet (s), doublet (d), triplet (t), quartet (q), multiplet (m), and broad (br).

Materials—Ethyl chloroformate (99%) and CaH_2 (60% in mineral oil), and 4-*tert* butyl benzyl alcohol (98%) were obtained from Acros Organic and used as received. 1,1,1-Tris(hydroxyl methyl)ethane (THME, 99%), triethylamine (TEA, 99%), 5-bromovaleryl chloride (98%) and CuBr (98%) were obtained from Alfa Aesar and used as received. Benzaldehyde (Aldrich 98%), *p*-toluene sulfonic acid (TsOH, Aldrich, 98.5%), (*N*, *N*′-bis [(3-trimethoxysilyl)propyl]ethylene diamine (enTMOS, 95% in MeOH, Gelest), tin(II) 2-ethyl hexanoate ($SnOct_2$ 98% MP Biomedicals), propargyl bromide (80% in toluene, TCI) and 3-aminopropyl trimethoxy silane (96% TCI) were used as received. L-Lactide was generously donated by Purac and used without further purification. Hexanes, acetone, chloroform, dichloromethane (DCM), anhydrous toluene, anhydrous methanol (MeOH), ethyl acetate and tetrahydrofuran (THF) were obtained from Fisher. THF was freshly distilled over sodium before use.

2.1 Synthesis of (Propargyl Carbonate (PC)) Monomer

Synthesis of PC monomer is adapted from previously reported work by Chen et al.[39] A typical synthesis of PC is presented and outlined in Scheme 1. THME (26 g, 0.217 mmol) and TsOH (1.2 g, 6.3 mmol) were dissolved in anhydrous THF (400 mL) and stirred at room temperature. To this stirring solution, benzaldehyde (23.2 mL, 0.23 mmol) was added dropwise and allowed to react for 16 hours. The reaction was then neutralized with aqueous ammonia and concentrated by rotary evaporation. The product was then dissolved in DCM and washed 3 times with water before again concentrating under rotary evaporation to yield 39 g (94%) of **C1** as a colorless solid. ^{1}H NMR (400 MHz, $CDCl_3$): δ 0.81 (s, 3H), 3.66 (d, 2H), 3.91 (s, 2H), 4.06 (d, 2H), 5.44 (s, 1H), 7.35–7.49 (m, 5H).

C1 (35 g, 168 mmol) in THF (50 mL) were added dropwise to a cold stirring solution of NaH (60% in mineral oil, 12 g, 302 mmol) at 0 °C to yield a milky white solution. After 30 minutes of cold stirring, the solution was heated on oil bath to 60 °C for 2 hours, yielding a pale yellow solution. Propargyl bromide (25 g, 211 mmol) was then added dropwise and allowed to stir for 16 hours. This solution was then quenched with water to afford a deep red solution with precipitate. This solution was extracted 3 times with brine and concentrated under high vacuum to yield crude **C2** as a red oil.

Crude **C2** (12 g, 48.7 mmol) was stirred in 400 mL 1:1 v/v MeOH:1M HCl for 2 hours. 1M NaOH was then used to raise the pH to 7 before MeOH was removed by rotary evaporation. The product was extracted using ethyl acetate to yield crude **C3**. Purification via flash chromatography using 2:1 ethyl acetate: hexanes yielded 6.1g (54% over 2 steps) **C3** as an orange oil. ^{1}H NMR (400 MHz, CDCl3): δ 0.84 (s, 3H), 1.65 (b, 2H) 2.45 (s, 1H) 3.49 (s, 2H) 3.58(d, 2H), 3.67(d, 2H), 4.15(s, 2H)

C3 was dissolved (5.18 g, 32.7 mmol) with ethyl chloroformate (6.68 g, 65 mmol) in THF (300 mL). Triethyl amine(7.1 g, 65 mmol) was then added to this stirring solution dropwise and allowed to react for 4 hours. Water was then used to quench the reaction slowly and the reaction was washed with brine. The organic layer was then concentrated by rotary evaporation and then purified via flash chromatography with 2:1 hexanes: ethyl acetate to yield 4.52 g (75%) Propargyl Carbonate (PC). ^{1}H NMR (400 MHz, CDCl3): δ 1.11 (s, 3H) 2.46 (s, 1H), 3.49(s, 2H), 4.07 (d, 2H), 4.17 (s, 2H) 4.33 (d, 2H). ^{13}C NMR (400 MHz, $CDCl_3$) δ 17.26, 32.8, 58.7, 70.66, 73.81, 75.25, 78.83, 148.17

2.2 Synthesis of Graft Monomer: 5-azido-*N*-(3-(trimethoxysilyl) propyl) pentanamide (AS)

Synthesis of AS is shown in Scheme 2. To a dry flask, (3-aminopropyl)trimethoxysilane (1.44 g, 8 mmol) were dissolved in THF with TEA (1 g, 10 mmol) and set to stir (clear solution). 5-bromovaleryl chloride (2 g, 10 mmol) was then added dropwise, forming a white precipitate. This solution was allowed to react for 16 hours under argon. The solution was subsequently filtered to remove the salt and concentrated by rotary evaporation to yield 2.73 g (99%) **G1** without further purification. ^{1}H NMR (400 MHz, CDCl3): δ 0.65 (q, 2H), 1.63 (p, 2H), 1.80 (m, 4H), 2.19 (t, 2H), 3.24 (t, 2H) 3.4 (t, 2H), 3.57 (s, 9H), 5.65 (b,1H)

G1 (2.73 g, 8 mmol) was then dissolved in anhydrous DMF and added to NaN_3 under dry conditions. This was allowed to react for 16 hours under argon atmosphere. DMF was then removed under vacuum for 36 hours before dry EtOAc was used to extract AS and the compound was again concentrated to yield pure AS 2.4 g (98%) which was stored under dry conditions in a glovebox. ^{1}H NMR (400 MHz, CDCl3): δ 0.65 (t, 2H), 1.78 (m, 6H), 2.19 (t, 2H), 3.26 (m, 4H), 3.41 (s, 9H), 5.69 (s, 1H). ^{13}CNMR (400MHz, $CDCl_3$) δ 6.46, 22.68, 22.81, 28.34, 35.83, 41.77, 50.45, 51.09, 172.27

2.3 Synthesis of Copolymers by $Sn(Oct)_2$ Catalyzed ROP

PC monomer was purified by flash chromatography and its purity was verified by NMR analysis. The monomer was dried over CaH_2 before use. Polymerization was carried out in toluene at 120 °C for 20 hours using 4-*tert*-butylbenzyl alcohol as the initiator and stannous-2-ethyl hexanoate ($Sn(Oct)_2$) as the catalyst (Scheme 3). The ratio of monomers to catalyst to initiator was 100:1:1 [M]:[C]:[I] for all polymerizations. The following is a typical synthesis for copolymer with 10 mol% PC loading. In a glovebox under argon atmosphere, LLA (7 g, 48 mmol) and PC (0.884 g, 4.8 mmol) were added to a high pressure flask with 10 mL anhydrous toluene. To this solution, $Sn(Oct)_2$ and 4-*tert*-butylbenzyl alcohol (0.075 M, 7 mL) were added quickly and the vessel was then sealed. The reaction container was quickly transferred to an oil bath outside of the glovebox and allowed to react

for 20 hours before quenching with methanol. The resulting polymer P(LLA-*co*-PC) was isolated by precipitation into cold MeOH, and further purified by precipitation from the DCM solution of the polymer into cold methanol 3 times. NMR analysis revealed this polymer to contain 6.4 mol% PC in the backbone and thus was denoted as P(LLA-*co*-PC) 6.4% for clarity.

2.4 Characterization of Polymers

The monomer incorporation ratio of all copolymers was determined using a Bruker spectrometer (400 MHz). $CDCl_3$ was used as the solvent and the chemical shifts were calibrated against residual solvent signals. The molecular weight and polydispersity of the copolymers were determined by a Waters 1515 gel permeation chromatograph (GPC) using THF as the eluent at a flow rate of 1.0 mL/min at 30 °C. A series of narrow polystyrene standards was used for the calibration of the columns. Thermal behavior was investigated using a TA Q100 differential scanning calorimeter (DSC) under nitrogen atmosphere. All samples were scanned from −10 °C to 200 °C at 10 °C/min before being quenched with liquid nitrogen. The samples were then rescanned from −10 °C to 200 °C and data were collected. Glass transition (T_g) was taken as the midpoint of heat capacity change and crystallization (T_c) and melting (T_m) were shown by exo- and endo-thermal peaks, respectively.

2.5 Post Polymerization Modification of Polymers via CuAAC

CuAAC reactions were performed in anhydrous DMF at room temperature under argon atmosphere. A typical synthesis of P(LLA-*co*-PC) 6.4% follows. The azide containing linking monomer (AS), was dissolved with P(LLA-*co*-PC) 6.4% and CuBr in DMF. Load ratios of AS to acetylene groups of the polymer were 1.1:1 (slight excess of AS) and CuBr was loaded at 2 mol%. Elemental copper was added in trace amounts to help stabilize Cu(I) ions in solution. This reaction is allowed to run for 2 hours before precipitation in cold MeOH to yield white powder of AS functionalized polymer P(LLA-*co*-PC)(AS) 6.4%. Polymers were treated with EDTA prior to precipitation in methanol to help remove excess copper catalyst.

2.6 Amalgamation of AS Functionalized Polymer

Composite cement materials were prepared for biaxial flexure and biocompatibility testing using P(LLA-*co*-PC)(AS)13.5% loaded at 10wt% into the composite A typical composite formation is presented here with 10 wt% copolymer in the composite. HAp-Gel (250 mg), prepared as previously reported[25], was mixed with P(LLA-*co*-PC)(AS)13.5% (25 mg) and the blend was ground into a fine powder. Next, 100 μL of enTMOS (95% in MeOH) was added to the powder and mixed thoroughly. To this mixture, a 10% acetone in PBS solution (420 μL) was added while gently kneading the composite into a clay. This clay was then formed into a mold and pressed to remove excess solvent. It was left for a minimum of 72 hours at room temperature to dry. This procedure was repeated for all composites. After drying, a solid material was obtained which could be trimmed and used to test the material's flexural strength.

2.7 Biaxial flexure strength

The testing procedure for biaxial flexure strength was performed according to Ban and Anusavice.[40] Four sample disks (diameter 10 mm by thickness 1mm) of each group (HAp-Gemosil and HAp-Gemosil/P(LLA-*co*-PC)AS 13.5%) were prepared in Teflon molds. The upper and lower surfaces were polished in order to obtain parallel surfaces with no apparent defects. After measuring the sample diameter (d) and thickness (t), the disk was supported on three stainless steel balls (3mm in diameter), which were equally spaced along a 3.25mm

radius (r_s). Prior to testing, a stainless steel piston (radius = r_p=1.5mm) was aligned concentrically with the three balls (Diagram 1). A crosshead speed of 0.5mm/min was used, and the maximum force at failure (P) was determined using an Instron 4411 Machine (model 4411, Instron Co., Norwood, MA). A Poisson's ratio (ν) of 0.3 was used for both materials. The flexure stress at failure (σ in MPa) was calculated using the following expressions: $\sigma = AP/t^2$ and $A = (3/4\pi)[2\,(1+\nu)\,\ln(r_s/r_o) + (1-\nu)\,(2\,r_s^2 - r_o^2)/2\,(d/2)^2 + (1+\nu)]$ where $r_o = (1.6\,r_p^2 + t^2)^{1/2} - 0.675t$.

2.8 Viability test-Preosteoblast cell proliferation by MTS Assay

The 6-well transwell plate (Corning Transwell-Clear Permeable Supports) was used for cell proliferation testing. The material disc (diameter 15mm by thickness 1mm) was placed on the permeable membrane support of the transwell, which allowed materials immersed in the culture medium. The 1×10^{-5} Preosteoblasts MC3T3-E1 were seeded to each well. Every three days, the medium was replenished with 2ml fresh growth medium (α-Minimum Essential Medium with 10% fetal bovine serum and 1% penicillin and streptomycin). At the end of cultivation (1, 7, and 21 days in culture), the disk and the permeable support were removed. 40 μL of 3-(4,5-dimethylthiazol-2-yl)-5-(3-carboxymethoxy-phenyl)-2-(4-sulfophenyl)-2H-tetrazolium salt (MTS) reagent (Promega, Madison, WI USA) was added to each well containing 400 μL of αMEM, and the plate was incubated for 1 hour at 37°C under a humidified atmosphere of 5% CO_2. From each well, 100 μL of the mixed solution was transferred into well of a 96-well plate. Each well was triplicated. The absorbance of each well at 490 nm was measured using a microplate reader (Microplate Reader 550, Bio-Rad laboratories, Philadelphia, USA). Relative cell numbers were quantified on the basis of the concentration of the formazan product of MTS. Three samples will be used at each time point for each material group. Three experimental groups of materials were investigated, including Gemosil, Gemosil/P(LLA-*co*-PC)AS 13.5%, and dishes as received without coating (control).

3. Results and Discussion

3.1 Monomer and Cross-Linker Synthesis

The hydrolysable cyclic carbonate monomer PC, was synthesized in four steps from established methods[39] as shown in Scheme 1. Due to the sensitive nature of both the azide and silane groups on the graft monomer molecule, azido-silane (AS), it is important to utilize a synthesis that would allow for highly pure products in nearly quantitative yields over all steps under mild conditions. To accomplish this, 5-Bromovaleryl chloride was first reacted with 3-aminopropyl trimethoxy silane to yield 5-bromo-*N*-(3-(trimethoxysilyl)propyl)pentanamide (**G1** in Scheme 2). An S_N2 reaction with sodium azide was then performed to yield 5-azido-*N*-(3-(trimethoxysilyl)propyl)pentanamide (AS, **G2** in Scheme 2). Both steps offered products in nearly quantitative yield with no need for purification as confirmed by NMR.

3.2 Synthesis and Characterization of Copolymers from $Sn(Oct)_2$ Catalyzed ROP

TMC homopolymer and PLLA have different physical properties,[18–19] therefore the percent incorporation of the PC unit (a TMC derivative) in the copolymer would impact important polymer properties such as molecular weight and T_g.[28,30–32,34] More importantly, these properties would determine whether or not the newly designed copolymers are suitable for specific applications.[17] Therefore, understanding the polymerization behavior and related properties of the copolymers precedes the development of composites. To accomplish this, we systematically varied the mol% PC in the load (0 – 100%) to investigate its effect on the polymerization and properties of the copolymer. This information would assist in future composite planning by helping elucidate the underlying chemistry that dictates polymer

properties, since these polymer properties will determine how polymers interact within a ceramic composite. The copolymerization was carried out at 120 °C in toluene and for 20 hours using an $Sn(Oct)_2$ catalyst and 4-*tert*-butylbenzyl alcohol as the initiator (Scheme 3). $Sn(Oct)_2$ was chosen because its versatility in ROP catalysis and ability to run at high temperature. 4-*tert*-butylbenzyl alcohol initiator was employed since its steric bulk can help inhibit intramolecular chain trans-esterification during polymerization. ^{1}H NMR was used to determine the ratio of incorporated carbonate to lactide in the polymer by comparing integrations of carbonate methyl (δ = 0.995 ppm) peaks and lactide methine (δ = 5.18 ppm) peaks, while GPC traces were taken from a THF solution of polymer to determine the molecular weight. The number averaged molecular weight (M_n) and %PC incorporation are plotted against the mol% PC loading in Figure 1A and B respectively. The most notable feature from Figure 1A is that the M_n decreases with the increased loading of the PC monomer, similarly observed by Gu et al. in a recent study.[31] Interestingly, the mol% incorporation of PC in the copolymer, shown in Figure 1B, is consistently lower than the mol% PC loading. Both of these observations can be attributed to the faster rate of polymerization of LLA compared with that of PC as previously reported for similar TMC-LLA copolymers.[30] Previous reports of lactide-carbonate copolymerizations showed that reaction times of >48 hours are needed to obtain high molecular weight copolymers that incorporated a high molar fraction of carbonate monomers.[31] However, at these elevated temperatures and reaction times, PLLA segments could thermally degrade more readily than polycarbonate segments.[30] In our cases, LLA is consumed faster than PC, resulting in a portion of PC monomers not being incorporated into the copolymer chain in the chosen reaction time (20 h). Instead, these unconsumed PC monomers form low molecular weight (MW) chains (2 – 4 kDa) consisting primarily of poly-propargyl carbonate, or remain as unreacted PC monomer. Due to the low MW and rubbery nature of PC, both remain soluble in methanol and are washed away during precipitation.

Detailed NMR analyses of all polymers elucidate further structural information of these polymers and the random nature of the copolymerization. To identify the chemical origin of each shift in the copolymers, a transition from PLLA homopolymer to PPC homopolymer with a P(LLA-*co*-PC)44.6% copolymer is shown in Figure 2A. The most interesting and diagnostic feature comes from the lactide protons (Figure 2B). In low mol %PC samples, a single peak is observed for the methine protons at δ = 5.18 ppm(proton **a** in Figure 2B). As the mol %PC increases, this methine signal begins to split, with a second peak appearing at δ = 5.02 ppm (proton **b** in Figure 2B). This secondary methine peak arises as a result of inductive effects on those methine peaks that neighbor a carbonate unit. These protons would feel a weaker de-shielding effect due to the lower electron withdrawing nature of the carbonate when compared with the ester in LLA, and thus will be shifted slightly upfield. This effect is observed only in LLA methine protons that are adjacent to a carbonate in the copolymer. During the copolymerization, if a propagating polymer chain end belongs to a lactide monomer and this “lactide” chain end opens up another lactide monomer, then all methine peaks are equivalent and no alternate shift is observed. When the propagating “lactide” chain end attacks a carbonate however, the additional oxygen on newly incorporated carbonate carbonyl helps slightly shield the α-methine proton that is next to the carbonate and leads to the appearance of a second peak upfield of the first (Figure 2A). This splitting effect is highlighted in Figure 2B. The relative ratio of these methine protons at different chemical shifts (5.18 ppm vs. 5.02 ppm) gradually decreases as the mol % PC increases in the copolymer, indicating the “random” nature of the copolymerization. A summary of polymer composition is given below in Table 1.

An important implication of employing the copolymer of LLA and PC is to lower the T_g of the copolymer. PLLA is below its T_g at the physiological temperature and the incorporation of PC into its backbone can help reduce crystallinity and lower the T_g of the resultant

copolymer. This provides a route for altering the crystallinity and helping to make the copolymer less brittle. This will allow for improved mechanical properties to be observed under physiological conditions and in turn, helping to raise flexural strength of future composites *in vivo*.[31,41] To demonstrate the impact on the T_g of the copolymer by the introduction of PC into PLLA, DSC traces of three polymers with different mol% incorporation of PC were obtained and compared (Figure 3). It is clearly observed that the T_g decreases with the increased PC content. Specifically, the T_g drops from 57.9 °C for PLLA, to 53.7 °C for P(LLA-co-PC)(AS)6.4%, and finally to 52.8 °C for P(LLA-co-PC)(AS)21%. The amorphous nature of the PC monomer helps to influence T_g by altering chain rigidity and hindering the chain's ability to pack effectively. Since both the HAp and enTMOS portions of the composite are very brittle, addition of a rubbery copolymer can help improve polymer tensile strength by increasing flexibility and elongation at break within the composite.[14]

PLLA and high PLLA content polymers appear as white fibrous solids at room temperature (0 – 10% PC incorporation) due to the high LLA content. As the mol% PC increases in the polymer, MW decreases and polymers becomes slightly more yellow in appearance, less fibrous and softer. Above 50 mol% PC incorporation, the polymers appear as viscous yellow/orange liquids. These polymers are largely amorphous due to the high PC content in the backbone, which serves to add steric bulk, reduce symmetry, and lower rigidity when compared with LLA segments. The short chain length of these polymers also obstructs effective packing and crystallization of adjacent chains. Examples of the physical appearance of several polymers are also given in Figure 3 for reference.

3.3 Post-Polymerization CuAAC Click Functionalization and Amalgamation

After determining that PC can successfully copolymerize with LLA to give polymers with controlled composition and properties, it was important to functionalize the pendant acetylene of PC to help understand how this functionalized polymer can be processed into HAp-Gemosil composites. CuAAC (a "Click" reaction) allows nearly quantitative coupling of terminal azides to alkynes via Cu(I) catalysis, with few byproducts and little purification needed.[42] This approach was attempted for several PC functionalized copolymers and coupling was observed to be successful.[10,43] However, after the CuAAC reaction, the recovery of polymer after attempted removal of residual copper catalyst proved difficult without initiating minor cross-linking of the grafted AS backbone groups. This cross-linking and subsequent loss of solubility confirmed the coupling reactions were successful. Fortunately, complete gelation was not observed for polymers with low mol %PC (<45%), due to the low density of AS on the backbone. However, the AS functionalized polymers showed poor solubility in PBS buffer and as-formed composites (i.e., copolymer mixed with HAp-Gel) showed poor properties after setting. To remedy this, 10% acetone in PBS buffer was used to facilitate dissolving P(LLA-*co*-PC)(AS) and subsequent blending the polymer with HAp-Gel to create a more homogenous composite. More importantly, using this two-solvent processing, the partially soluble white powder formed after CuAAC can now be further reacted through these un-crosslinked, free alkoxysilyl groups with another silane containing cross-linking reagent, enTMOS, for better setting. The use of enTMOS allows rapid condensation of trialkoxy silanes, to rapidly form a strong cross-linked composite. In our investigation, this functionalized polymer powder is finely ground with HAp-Gel and blended with enTMOS, allowing enTMOS to bond to free siloxane groups of P(LLA-*co*-PC)(AS). This reaction incorporates the newly prepared copolymer into the composite siloxane matrix through enTMOS. This multiple crosslinking via enTMOS creates a fully linked gel which can be easily formed and allows for chemical linking of polymer to HAp-Gel to enTMOS, increasing long range adhesion and strength.

After successfully forming these new composites with our designed copolymers incorporated, we then carried out the cellular and mechanical studies to determine the effect that polymer blending has on composites when compared with previously studied HAp-Gemosil samples. Figure 4 presents the results of the 21 day MTS assay, It can be seen from these data that, when compared with the control sample, both previous HAp-Gemosil and new HAp-Gemosil/P(LLA-*co*-PC)(AS) composites showed similar biocompatibility over a 21 day period. Furthermore, the resultant growth curves of MC3T3-E1 cells were similar for all three groups. Cells grew up to 7 days and, then, leveled out. There were no differences in absorbance between the materials and the control, showing no difference in cell viability among the tested substrates. These data suggest that the incorporation of P(LLA-*co*-PC)(AS) had little to no negative effect on the biocompatibility of these composites, and minimal toxic byproducts leaching out from this composite by 21 days.

As previously mentioned, HAp-Gemosil composites lacked sufficient flexural strength for use in orthopedic applications. The incorporation of a cross-linkable polymer was expected to help improve long range interaction within the composite. As presented in Figure 5, the higher flexure strength of HAp-Gemosil/P(LLA-*co*-PC)(AS) composites than that of the original HAp-Gemosil indicates an effect of fiber bridging coming from the blended long chain copolymers. The stiffness of the force-displacement curve recorded from the biaxial bending test did not differ (P=0.08) between the original (2.06 N/mm) and the new (2.15 N/mm) composites. In our in-house data, the HAp-Gemosil had a compressive modulus around 862±129 MPa and a reduced modulus 18.0±4.9 GPa measured by the nanoindentation tester (Hysitron Inc.) Based on the stiffness data, we expect that the new composite might have similar modulus values although future tests are required.

Though the results from initial biocompatibility and mechanical tests are promising, this polymer system presents several key limitations. Primarily, the sensitivity of the P(LLA-*co*-PC)(AS) lead to premature cross-linking of polymer bound silanes. This in turn made complete blending of composite cements with the polymer more difficult. This limitation can influence reproducibility and utility of composites like those tested in this study. The use of a second, less polar solvent (acetone) during blending helped improve composite formation, making it possible to study the interaction of this polymer within HAp-Gemosil composites. Unfortunately, the use of organic solvents removes our ability to dope this composite with cells for scaffolding applications, and these processing issues hinder the ability to study composite interactions *in vivo*. Despite the drawbacks, this system still showed merit in improving the properties of HAp-Gemosil composites, while preserving their biocompatibility. Improvements in cross-linking chemistry are required to allow for better processibility and material performance. These improvements would allow this system to be more rigorously studied *in vivo* to determine the efficacy of this polymer/ceramic system for future scaffolding applications.

4. Conclusions

In summary, we have synthesized a derivatized TMC monomer, PC, which is capable of undergoing ROP with L-Lactide to afford copolymers with tunable MW, mol % PC incorporation and T_g. The ability of these monomers to copolymerize and yield potentially biodegradable and biocompatible polymers of tunable properties makes this an attractive system for biological applications. In the current demonstration, we coupled the copolymer with AS graft agents inspired by enTMOS, converting the copolymer into “cross-linkable” via these pendant silane groups. After being processed into the original HAp-Gemosil cement composite facilitated by the amino-silane enTMOS, these AS functionalized polymers were capable of bridging the new composite and providing enhanced long range adhesion, while still maintaining the biocompatibility of the new composite.

The current grafting approach did have some key limitations, however. Notably, the sensitivity of polymer bound silanes prevented extensive purification after CuAAC coupling. As a result, some residual copper from CuAAC was generally trapped in the composite after coupling, which could lead to the possibility of increased cell morbidity. Furthermore, the premature cross-linking could contribute to an inability of these polymers to fully cross-link into the enTMOS silsesquioxane matrix, leading to poor adhesion between the hydrophobic polymer and the hydrophilic HAp-Gel moieties in the composite. Therefore, further work remains to be done, especially regarding the graft monomer and cross-linking. Fortunately, the PC monomer introduces a pendant acetylene group on the copolymer, which provides a synthetic handle for post-polymerization modification to give more synthetic freedom. This ‘acetylene handle’ allows various pendant groups to be attached to the copolymer, thus one can further alter the composite properties to obtain unique, applications specific properties. Future composites will be synthesized using similar P(LLA-*co*-PC) polymers as the chemistry and properties of these copolymer have been elucidated in this study, but emphasis will be placed on utilizing alternate “click” reactions which can preclude the use of potentially toxic catalysis. Alternate graft monomers will also be investigated to determine a method for cross-linking which can be easily degraded. This will eliminate potential problems caused by residual material left after degradation. Additionally, a less sensitive method of cross-linking would be ideal as to allow better control of cross-linking reactions and thereby improve processing of the final composite. If these issues can be sufficiently addressed, this HAp-Gemosil-P(LLA-co-PC)(AS) copolymer system will provide a new springboard to undertake further scaffolding composite work.

Supplementary Material

Refer to Web version on PubMed Central for supplementary material.

Acknowledgments

The authors acknowledge funding from NC Biotech Grant #2008-MRG-1108, NIH/NIDCR, K08DE018695 American Association of Orthodontist Foundation, and UNC University Research Council. We thank Wonhee Jeong for many useful discussions regarding our work and John Whitley for his assistance in characterizing and testing polymers and composites. Additionally we thank Purac Biomaterials for their generous donation of L-Lactide for this project.

References

1. Field RA, Riley ML, Mello FC, Corbridge JH, Kotula AW. Bone Composition in Cattle, Pigs, Sheep and Poultry. J Anim Sci. 1974; 39(3):493–499. [PubMed: 4412232]
2. Puppi D, Chiellini F, Piras AM, Chiellini E. Polymeric materials for bone and cartilage repair. Progress in Polymer Science. 2010; 35(4):403–440.
3. Shoichet MS. Polymer Scaffolds for Biomaterials Applications. Macromolecules. 2009; 43(2):581–591.
4. Bongio M, van den Beucken JJJP, Leeuwenburgh SCG, Jansen JA. Development of bone substitute materials: from ‘biocompatible’ to ‘instructive’. Journal of Materials Chemistry. 2010; 20(40): 8747–8759.
5. Imam Khasim HR, Henning S, Michler GH, Brand J. Development of Nanocomposite Scaffolds for Bone Tissue Engineering. Macromolecular Symposia. 2010; 294(1):144–152.
6. Rezwan K, Chen QZ, Blaker JJ, Boccaccini AR. Biodegradable and bioactive porous polymer/ inorganic composite scaffolds for bone tissue engineering. Biomaterials. 2006; 27(18):3413–3431. [PubMed: 16504284]
7. Roether JA, Boccaccini AR, Hench LL, Maquet V, Gautier S, Jérôme R. Development and in vitro characterisation of novel bioresorbable and bioactive composite materials based on polylactide

foams and Bioglass® for tissue engineering applications. Biomaterials. 2002; 23(18):3871–3878. [PubMed: 12164192]

8. Declercq H, Cornelissen M, Gorskiy T, Schacht E. Osteoblast behaviour on *in situ* photopolymerizable three-dimensional scaffolds based on D, L-lactide, ε-caprolactone and trimethylene carbonate. Journal of Materials Science: Materials in Medicine. 2006; 17(2):113–122. [PubMed: 16502243]
9. Oh JK. Polylactide (PLA)-based amphiphilic block copolymers: synthesis, self-assembly, and biomedical applications. Soft Matter. 2011; 7(11):5096–5108.
10. Jiang X, Vogel EB, Smith MR, Baker GL. "Clickable" Polyglycolides: Tunable Synthons for Thermoresponsive, Degradable Polymers. Macromolecules. 2008; 41(6):1937–1944.
11. Shokrollahi P, Mirzadeh H, Scherman OA, Huck WTS. Biological and mechanical properties of novel composites based on supramolecular polycaprolactone and functionalized hydroxyapatite. Journal of Biomedical Materials Research Part A. 2010; 95A(1):209–221. [PubMed: 20574978]
12. Zhou Y, Hutmacher DW, Varawan S-L, Lim TM. In vitro bone engineering based on polycaprolactone and polycaprolactone–tricalcium phosphate composites. Polymer International. 2007; 56(3):333–342.
13. Bat E, van Kooten TG, Feijen J, Grijpma DW. Crosslinking of Trimethylene Carbonate and D, L-Lactide (Co-) Polymers by Gamma Irradiation in the Presence of Pentaerythritol Triacrylate. Macromolecular Bioscience. 2011; 11(7):952–961. [PubMed: 21480530]
14. Andronova N, Albertsson A-C. Resilient Bioresorbable Copolymers Based on Trimethylene Carbonate, l-Lactide, and 1,5-Dioxepan-2-one. Biomacromolecules. 2006; 7(5):1489–1495. [PubMed: 16677030]
15. Dargaville BL, Vaquette C, Peng H, Rasoul F, Chau YQ, Cooper-White JJ, Campbell JH, Whittaker AK. Cross-Linked Poly(trimethylene carbonate-co-l-lactide) as a Biodegradable, Elastomeric Scaffold for Vascular Engineering Applications. Biomacromolecules. 2011; 12(11): 3856–3869. [PubMed: 21999900]
16. Jiang T, Nukavarapu SP, Deng M, Jabbarzadeh E, Kofron MD, Doty SB, Abdel-Fattah WI, Laurencin CT. Chitosan-poly(lactide-co-glycolide) microsphere-based scaffolds for bone tissue engineering: In vitro degradation and in vivo bone regeneration studies. Acta Biomaterialia. 2010; 6(9):3457–3470. [PubMed: 20307694]
17. Bat E, Plantinga JeA, Harmsen MC, van Luyn MJA, Zhang Z, Grijpma DW, Feijen J. Trimethylene Carbonate and ε-Caprolactone Based (co)Polymer Networks: Mechanical Properties and Enzymatic Degradation. Biomacromolecules. 2008; 9(11):3208–3215. [PubMed: 18855440]
18. Middleton JC, Tipton AJ. Synthetic biodegradable polymers as orthopedic devices. Biomaterials. 2000; 21(23):2335–2346. [PubMed: 11055281]
19. Hench LL. Prosthetic Implant Materials. Annual Review of Materials Science. 1975; 5(1):279–300.
20. Mukherjee S, Gualandi C, Focarete M, Ravichandran R, Venugopal J, Raghunath M, Ramakrishna S. Elastomeric electrospun scaffolds of poly(<small>l</small>-lactide-*co*-trimethylene carbonate) for myocardial tissue engineering. Journal of Materials Science: Materials in Medicine. 2011; 22(7):1689–1699. [PubMed: 21617996]
21. Zheng L, Yang F, Shen H, Hu X, Mochizuki C, Sato M, Wang S, Zhang Y. The effect of composition of calcium phosphate composite scaffolds on the formation of tooth tissue from human dental pulp stem cells. Biomaterials. 2011; 32(29):7053–7059. [PubMed: 21722953]
22. Chang MC, Ko C-C, Douglas WH. Preparation of hydroxyapatite-gelatin nanocomposite. Biomaterials. 2003; 24(17):2853–2862. [PubMed: 12742723]
23. Ko CCOM, Fallgatter AM, Hu W-S. Mechanical properties and cytocompatibility of biomimetic hydroxyapatite-gelatin nanocomposites. J Material Research. 2006; 21(12):8.
24. Ko, CC.; WY-L; Douglas, WH.; Narayanan, R Edi; Aizenberg, J.; Landis, WJ.; Orme, C.; Wang, R.; Hu, W-S. In Vitro And In Vivo Tests Of Hydroxyapatite-Gelatin Nanocomposites For Bone Regeneration: A Preliminary Report. Biological and Bioinspired Materials and Devices; Symposium Proceedings Material Research Society Spring Meeting; 2004. p. 5

25. Luo T-J, Ko C-C, Chiu C-K, Llyod J, Huh U. Aminosilane as an effective binder for hydroxyapatite-gelatin nanocomposites. Journal of Sol-Gel Science and Technology. 2010; 53(2): 459–465.
26. Deng X, Hao J, Wang C. Preparation and mechanical properties of nanocomposites of poly(,-lactide) with Ca-deficient hydroxyapatite nanocrystals. Biomaterials. 2001; 22(21):2867–2873. [PubMed: 11561892]
27. Todo M, Kagawa T. Improvement of fracture energy of HA/PLLA biocomposite material due to press processing. Journal of Materials Science. 2008; 43(2):799–801.
28. Zhang L, Goh SH, Lee SY. Miscibility and crystallization behaviour of poly(-lactide)/poly(p-vinylphenol) blends. Polymer. 1998; 39(20):4841–4847.
29. Zhang C, Subramanian H, Grailer JJ, Tiwari A, Pilla S, Steeber DA, Gong S. Fabrication of biodegradable poly(trimethylene carbonate) networks for potential tissue engineering scaffold applications. Polymers for Advanced Technologies. 2009; 20(9):742–747.
30. Ruckenstein E, Yuan Y. Molten ring-open copolymerization of L-lactide and cyclic trimethylene carbonate. Journal of Applied Polymer Science. 1998; 69(7):1429–1434.
31. Ji L-J, Lai K-L, He B, Wang G, Song L-Q, Wu Y, Gu Z-W. Study on poly(l-lactide -co-trimethylene carbonate): synthesis and cell compatibility of electrospun film. Biomedical Materials. 2010; 5(4):045009. [PubMed: 20644241]
32. Tyson T, Finne-Wistrand A, Albertsson A-C. Degradable Porous Scaffolds from Various l-Lactide and Trimethylene Carbonate Copolymers Obtained by a Simple and Effective Method. Biomacromolecules. 2008; 10(1):149–154. [PubMed: 19063595]
33. Nederberg F, Lohmeijer BGG, Leibfarth F, Pratt RC, Choi J, Dove AP, Waymouth RM, Hedrick JL. Organocatalytic Ring Opening Polymerization of Trimethylene Carbonate. Biomacromolecules. 2006; 8(1):153–160. [PubMed: 17206801]
34. Vandenberg EJ, Tian D. A New, Crystalline High Melting Bis(hydroxymethyl)polycarbonate and Its Acetone Ketal for Biomaterial Applications. Macromolecules. 1999; 32(11):3613–3619.
35. Durucan C, Brown PW. Biodegradable Hydroxyapatite–Polymer Composites. Advanced Engineering Materials. 2001; 3(4):227–231.
36. Hoffmann F, Cornelius M, Morell J, Fröba M. Silica-Based Mesoporous Organic–Inorganic Hybrid Materials. Angewandte Chemie International Edition. 2006; 45(20):3216–3251.
37. Lutz J-F. 1,3-Dipolar Cycloadditions of Azides and Alkynes: A Universal Ligation Tool in Polymer and Materials Science. Angewandte Chemie International Edition. 2007; 46(7):1018–1025.
38. Binder WH, Sachsenhofer R. ‘Click’ Chemistry in Polymer and Materials Science. Macromolecular Rapid Communications. 2007; 28(1):15–54.
39. Chen W, Yang H, Wang R, Cheng R, Meng F, Wei W, Zhong Z. Versatile Synthesis of Functional Biodegradable Polymers by Combining Ring-Opening Polymerization and Postpolymerization Modification via Michael-Type Addition Reaction. Macromolecules. 2010; 43(1):201–207.
40. Ban S, Anusavice KJ. Influence of Test Method on Failure Stress of Brittle Dental Materials. Journal of Dental Research. 1990; 69(12):1791–1799. [PubMed: 2250083]
41. Valliant EM, Jones JR. Softening bioactive glass for bone regeneration: sol-gel hybrid materials. Soft Matter. 2011; 7(11):5083–5095.
42. Kolb HC, Finn MG, Sharpless KB. Click Chemistry: Diverse Chemical Function from a Few Good Reactions. Angewandte Chemie International Edition. 2001; 40(11):2004–2021.
43. Parrish B, Breitenkamp RB, Emrick T. PEG-and Peptide-Grafted Aliphatic Polyesters by Click Chemistry. Journal of the American Chemical Society. 2005; 127(20):7404–7410. [PubMed: 15898789]

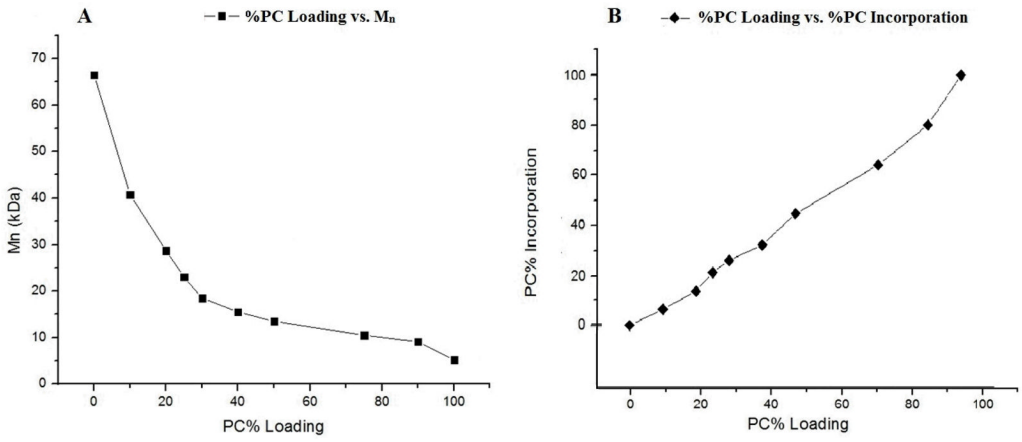

Figure 1.

(A) Polymer molecular weight (M_n) as a function of increasing %PC load. (B) %PC present in the polymer chain as a function of mol fraction loaded before polymerization.

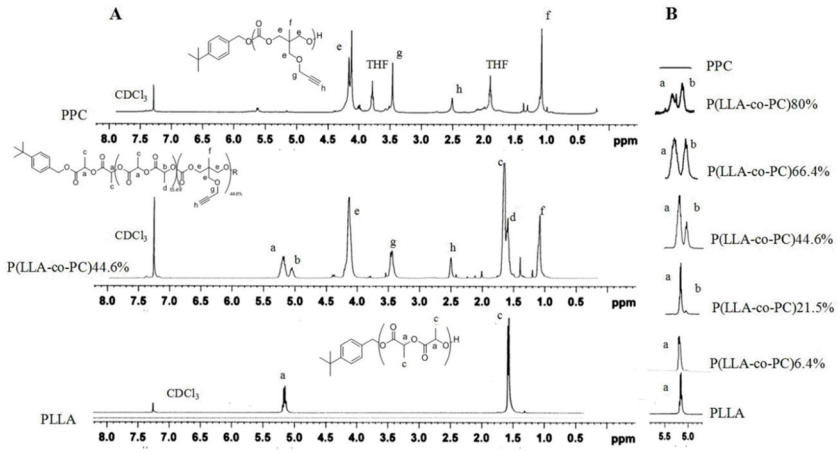

Figure 2.

(A) The NMR spectra of homopolymers with a P(LLA-*co*-PC)44.6% copolymer. (B) The splitting observed from lactide methine peaks for copolymers of varied %PC loadings.

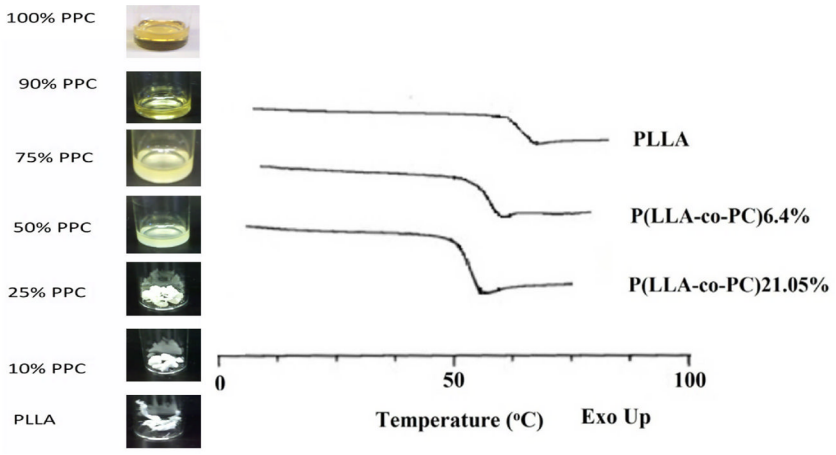

Figure 3.

Left: Images of several polymers to demonstrate changes in physical appearance caused by changes in polymer chain length and distribution. Right: DSC traces for three of these polymers are given to demonstrate the tunability of T_g as a function of increased %PC content on the polymer backbone.

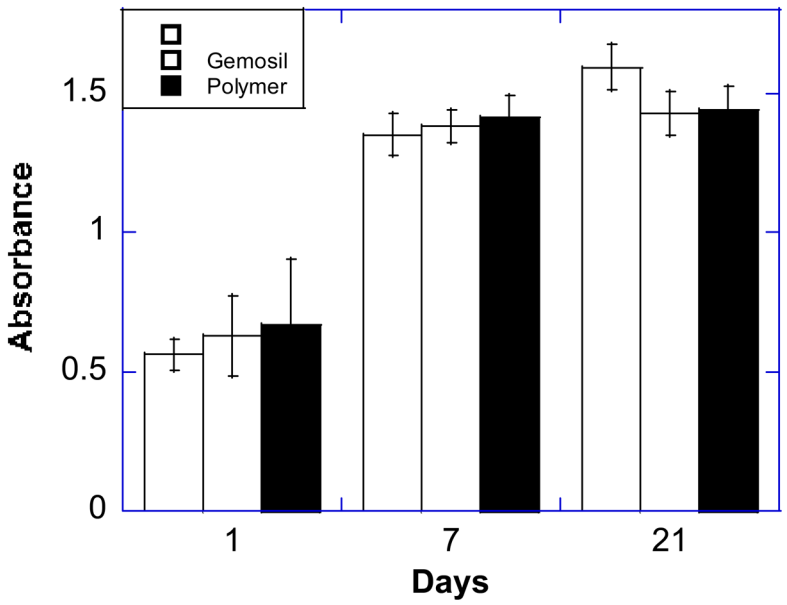

Figure 4.
Cell viability data for cells plated on both HAp-Gemosil and Polymer(AS) 13.5%. Cells were plated in 96 well plates and viability was measured by formazan absorbance at Days 1, 7, and 21

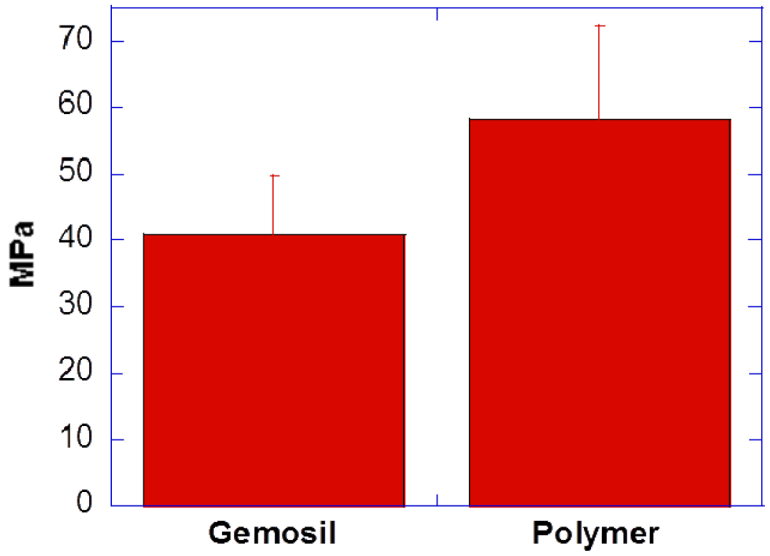

Figure 5.
Changes in UTS between HAp-Gemosil and HAp-Gemosil doped with P(LLA-*co*-PC)AS polymers.

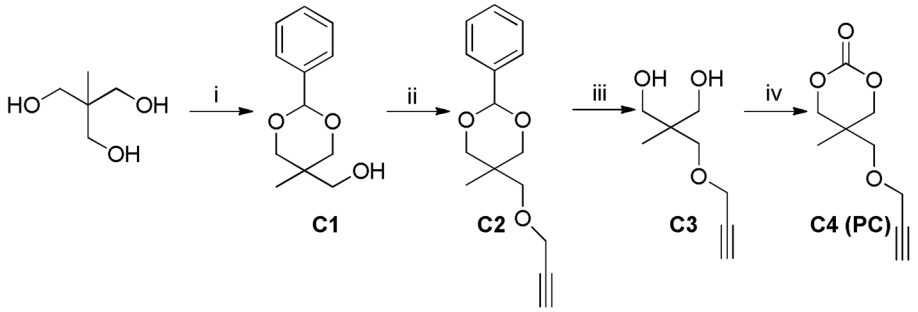

Scheme 1.

Synthesis of C4 (PC) from THME

Reaction Conditions for synthesis of PC from THME: (i) benzaldehyde, TsOH, THF; (ii) NaH, Propargyl bromide, THF; (iii) MeOH: 1M HCl (1:1, v:v); (iv) THF, ethyl chloroformate, TEA.

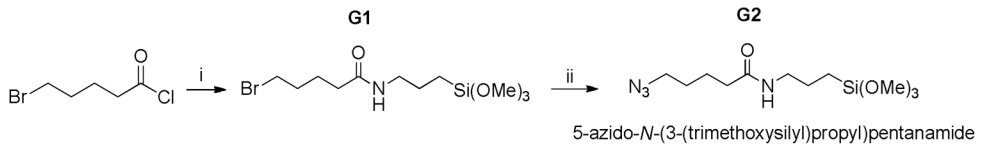

Scheme 2.

Synthesis of AS

Reaction conditions for synthesis of AS: (i)3-aminopropyl trimethoxy silane, TEA, THF; (ii) DMF, NaN_3.

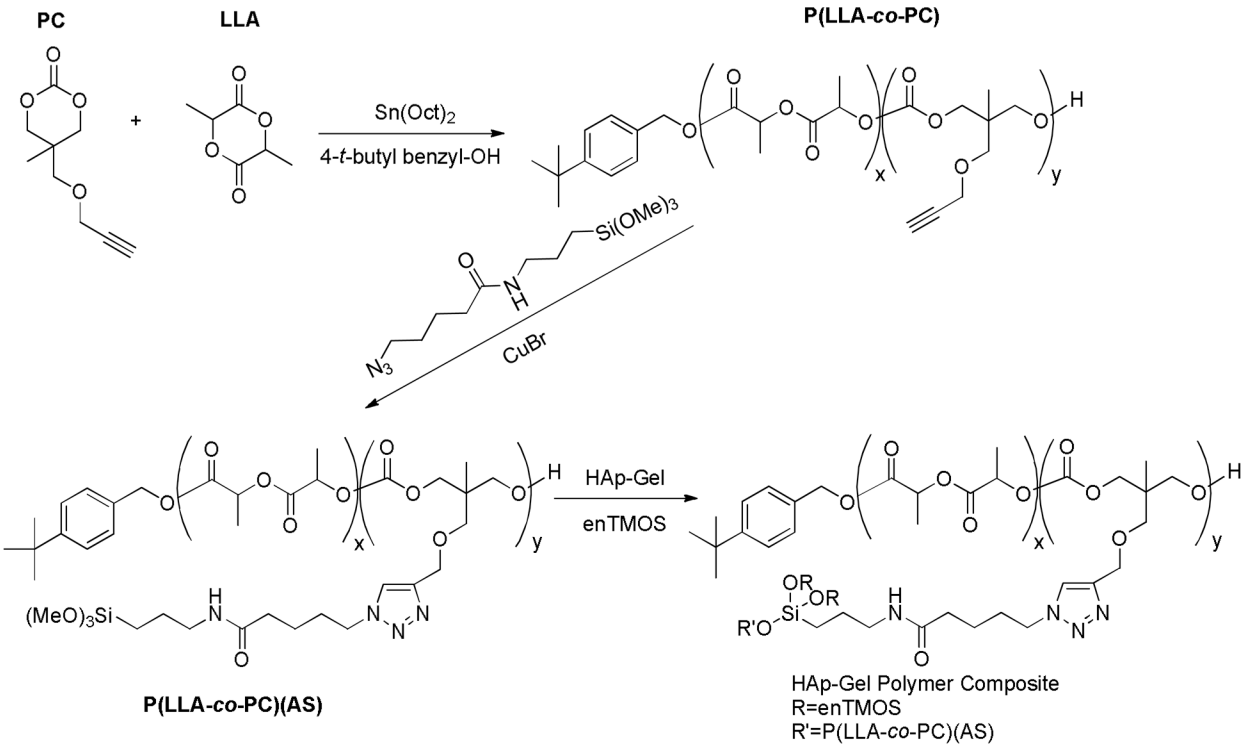

Scheme 3.

ROP of LLA and PC, CuAAC Modifications and Amalgamation[a]

[a] Scheme 3 shows ROP polymer formation, followed by CuAAC post-polymerization modification before processing into enTMOS HAp-Gel composite cement. This cement is stabilized by polymer bridging and cross-linking through the AS trialkoxysilyl moiety. This silane network will bind HAp, enTMOS, and neighboring polymer chains to increase long range adhesion and strength.

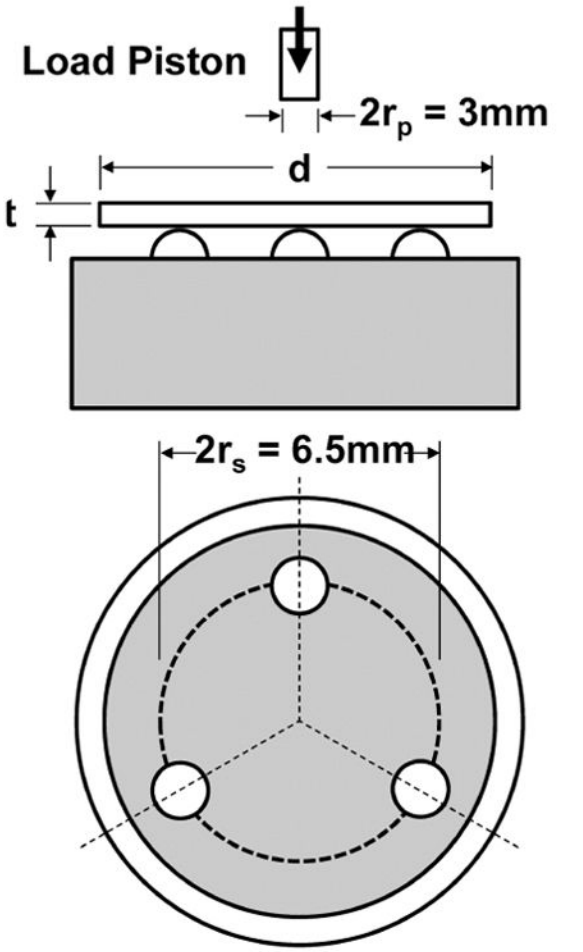

Diagram 1.
Biaxial flexure test apparatus.

Table 1

Summarized polymerization data for P(LLA-*co*-PC) copolymers.

PC Loading (%PC)[a]	%PC Incorporation[b]	M_n (kDa)[c]	M_w (kDa)
0	0	66.7	93.7
10	6.4	53.0	57.8
20	13.5	28.7	46.6
25	21.05	23.0	35.8
30	25.9	18.6	33.5
40	32.1	15.5	23.3
50	44.6	13.5	22.6
75	64.1	10.5	12.4
90	80	9.1	11.3
100	100	5.2	9.4

[a] Copoymers of LLA and PC, denote by the % loading of PC during polymerization

[b] Incorporation measured by H^1 NMR

[c] Measured by GPC with THF eluent